

Monitoring Lévy-Process Crossovers

Maike A. F. dos Santos¹, Fernando D. Nobre¹, and Evaldo M. F. Curado¹

¹*Centro Brasileiro de Pesquisas Físicas and National Institute of Science and Technology for Complex Systems, Rua Xavier Sigaud 150, Rio de Janeiro, RJ 22290-180, Brazil*

Abstract

The crossover among two or more types of diffusive processes represents a vibrant theme in nonequilibrium statistical physics. In this work we propose two models to generate crossovers among different Lévy processes: in the first model we change gradually the order of the derivative in the Laplacian term of the diffusion equation, whereas in the second one we consider a combination of fractional-derivative diffusive terms characterized by coefficients that change in time. The proposals are illustrated by considering semi-analytical (i.e., analytical together with numerical) procedures to follow the time-dependent solutions. We find changes between two different regimes and it is shown that, far from the crossover regime, both models yield qualitatively similar results, although these changes may occur in different forms for the two models. The models introduced herein are expected to be useful for describing crossovers among distinct diffusive regimes that occur frequently in complex systems.

Keywords: Fractional Dynamics, Fractional Calculus, Stochastic processes, Lévy flights, Non-Gaussian distributions.

1. Introduction

According to Einstein's theory, the problem of Brownian motion may be seen as a diffusion of Brownian particles through a homogeneous environment. Consequently, it follows the linear diffusion equation [1, 2],

$$\frac{\partial p(x, t)}{\partial t} = D \frac{\partial^2 p(x, t)}{\partial x^2} , \quad (1)$$

where D is the diffusion constant and $p(x, t)$ represents a continuous probability density for finding the tagged particle in a position between x and $x + dx$, at time t (for simplicity, we restrict ourselves to a one-dimensional space). The well-known solution of this equation is the Gaussian distribution,

$$p(x, t) = \frac{1}{(4\pi Dt)^{1/2}} \exp[-x^2/(4Dt)] , \quad (2)$$

so that the mean-square displacement,

$$\langle (\Delta x)^2 \rangle = 2Dt , \quad (3)$$

increases linearly with t , a typical signature of the Brownian motion and all linear-diffusion processes.

However, nowadays a wide variety of systems has presented non-Gaussian distributions [1, 2, 3, 4], which may be found as natural consequences of several theoretical studies, like nonextensive statistical mechanics [4, 5], superstatistics [6, 7, 8], diffusion with memory kernels [9, 10, 11], controlled diffusion [12, 13, 14], rare events [15, 16], and nonlinear Fokker-Planck equations [17, 18, 19, 20, 21, 22]. To take into account non-Gaussian distributions, essentially two distinct procedures have been mostly proposed in the literature, for generalizing the linear-diffusion equation in Eq. (1), as described next. (i) In the first approach, one keeps the standard derivatives and introduces nonlinearities in the probability $p(x, t)$; the most known case leads to the porous-medium equation, where one introduces a power in the probability of the diffusion term [4, 17]. By adding an extra contribution in the porous medium equation, due to an external confining potential, one obtains a nonlinear Fokker-Planck equation [18, 19, 20, 21, 22]. These types of nonlinear equations present solutions known in the literature as q -Gaussian distributions [which recover the Gaussian of Eq. (2) in the limit $q \rightarrow 1$], being intimately related to nonextensive statistical mechanics, leading to

a wide variety of applications in social, economical, physical, and biological systems [4, 5, 17, 18, 19, 20, 21, 22, 23]. (ii) In the second procedure, one keeps the probability linear, but turn the standard derivatives into fractional derivatives [24, 25, 26]. More particularly, by introducing a fractional derivative in the diffusion term, the corresponding solutions are known as Lévy distributions [27, 28, 29, 30, 31, 32]. In the present investigation we restrict ourselves to this second approach; according to this later scenario, the non-Gaussian distributions are connected with anomalous-diffusion processes, through a power-law behavior in the mean-square displacement, i.e. $\langle(\Delta x)^2\rangle = 2\mathcal{K}_\alpha t^\alpha$ ($\alpha > 0$), where \mathcal{K}_α represents a general diffusion coefficient with fractional dimension. Actually, such relation is usually associated with various diffusive behaviors [26, 25], classified as sub- ($0 < \alpha < 1$), normal- ($\alpha = 1$), super- ($1 < \alpha < 2$), and hyper- ($\alpha > 2$) diffusive processes; the particular case $\alpha = 2$ is known as ballistic diffusion.

Many studies in the literature were dedicated to Lévy statistics [27, 24], and the so-called Lévy distributions, which became powerful tools to approach some complex systems [28, 29]. The most general form of a Lévy distribution is written in terms of two indexes, $L_{\mu,\beta}(z)$, where μ is a real exponent (to be defined below) and β represents an asymmetry parameter [2]; herein, we will deal with symmetric Lévy distributions, corresponding to $\beta = 0$. Hence, for simplicity, we define $L_\mu(z) \equiv L_{\mu,0}(z)$, expressed in terms of the following Fourier transform,

$$L_\mu(z) = \frac{1}{2\pi} \int_{-\infty}^{\infty} e^{ikz - a|k|^\mu} dk . \quad (4)$$

The integral above is nonnegative for $0 < \mu \leq 2$ and consequently it may be considered as a probability density only in this range [1]; it recovers the Gaussian and Cauchy distributions in the particular limits $\mu = 2$ and $\mu = 1$, respectively. For $0 < \mu < 2$, these distributions present power-law tails, $L_\mu(z) \sim z^{-(1+\mu)}$, leading to a divergence in the mean-square displacement, $\langle(\Delta z)^2\rangle \rightarrow \infty$ [3, 30].

From the theoretical point of view, the Lévy distribution appears in a generalized version of central-limit theorem, where the sum of identically distributed random variables follows power laws, instead of a Gaussian distribution [31, 32]. In the scenario of the fractional Fokker-Planck equation [24], the fractional diffusion can be constructed through the Scher-Montroll equation [33, 34, 35], where a particular case is expressed in terms of the Riesz

derivative, presenting the Lévy distribution as a solution. The Riesz fractional derivative has found applications that go beyond statistical mechanics, e.g., in a fractional Schrödinger equation [36] that appears as a potential model to explain some laser measurements [37, 38]. Moreover, the Lévy distributions were found in fractional-collision models (Rayleigh, driven Maxwell gas) [39, 40], models with single big jumps [41], cold atoms trapped in optical lattices [42], and stochastic resetting processes [43].

Nowadays the fractional dynamics (in Riesz sense) has become an useful tool for describing the protein sliding in polymeric systems (e.g., DNA) [44]. In these situations the occurrence of a single big jump is associated with the protein folding. Thereby, the dynamics for a single type of Lévy process can be defined by a continuous probability $p(x, t)$ following

$$\frac{\partial p(x, t)}{\partial t} = \frac{\partial^\mu p(x, t)}{\partial |x|^\mu} . \quad (5)$$

One should notice that the equation above suggests a scaling between position and time, i.e., $|x| \sim t^{1/\mu}$; therefore, the solution of Eq. (5) is expressed in terms of a Lévy distribution,

$$p(x, t) = \frac{1}{t^{\frac{1}{\mu}}} L_\mu \left[\frac{|x|}{t^{\frac{1}{\mu}}} \right] . \quad (6)$$

It is well known that protein walks in DNA play an important role in reparation of some genetic sequences [45] that include mutations or chromosomal defects. In this scenario, the dynamic behavior of proteins in DNA can be described by a search-for-target model [44]; this model includes a fractional Laplacian term (like in Eq. (5)) to take into account the big jumps among different parts of DNA folds. Within this context, one can think of the possibility for a given walker to be governed by two different Lévy processes in distinct time regimes. Similar situations, exhibiting crossovers between anomalous to normal diffusion processes, have been observed in telomeres in the nucleus of mammalian cells [46], diffusion in biological cells [47], as well as in various complex systems [48, 49, 50, 51, 52, 53].

However, a theoretical support for crossovers between different Lévy processes remains open. In the present work we investigate this question by proposing two models that may exhibit such kind of phenomenon, presenting

the ability to generate crossovers among different Lévy processes described through the fractional Riesz derivative. In section 2 we introduce the two models: (i) In the first one we change gradually the order of the derivative in the Laplacian term of the diffusion equation; (ii) In the second one we consider a combination of fractional-derivative diffusive terms characterized by coefficients that change in time. In both cases we work out analytical time-dependent solutions; then, we illustrate typical crossovers by following numerically the time evolution of the probability distribution. It is shown that, far from the crossover regime, both models yield qualitatively similar results, although the changes may occur in different forms for the two models. Finally, in section 3 we present our main conclusions and discuss possible applications for the models introduced.

2. Models for crossovers between Lévy processes

Let us consider a random walk, exhibiting a crossover in time, described by a normalized continuous probability,

$$\int_{-\infty}^{\infty} dx p(x, t) = 1 \quad (\forall t), \quad (7)$$

following Lévy processes according to Eq. (5). The crossover is signalled by two different exponents μ_1 ($t \ll t_{\text{cross}}$) and μ_2 ($t \gg t_{\text{cross}}$), where t_{cross} represents a typical time for the change between the two regimes to occur. Next we propose two models that produce crossovers among Lévy flights. The first one considers the fractional derivative in the Laplacian term of the diffusion equation with a variable order, whereas the second one is defined by two fractional-derivative diffusive terms, each of them multiplied by different time-dependent diffusion coefficients.

2.1. Model 1: Time-Dependent Order of the Fractional Derivative

The idea of fractional-differential operators with variable order was introduced recently [54, 55], leading to an increasingly interest and various applications, like anomalous diffusion [56, 57], memory modelling [58], reaction-diffusion problems [59], wave equation [60], telegraph equation [61, 62], and other investigations [63, 64, 65, 66, 67, 68].

Herein, we adopt the following time-dependent-order Riesz fractional-derivative definition for a two-variable function $f(x, t)$ [69, 70],

$$\frac{\partial^{\mu(t)} f(x, t)}{\partial |x|^{\mu(t)}} = b[\mu(t)] \int_0^{+\infty} d\xi \frac{f(x + \xi, t) - 2f(x, t) + f(x - \xi, t)}{\xi^{1+\mu(t)}} , \quad (8)$$

where $b[\mu(t)] = \frac{\Gamma(1+\mu(t))}{\pi} \sin\left(\frac{\mu(t)\pi}{2}\right)$ and $1 \leq \mu(t) \leq 2$. A numerical analysis of the definition above was carried in Ref. [70], showing its stability and convergence in the diffusion equation. The Fourier transform of this derivative is expressed as

$$\mathcal{F} \left\{ \frac{\partial^{\mu(t)}}{\partial |x|^{\mu(t)}} f(x, t) \right\} = -|k|^{\mu(t)} f(k, t) , \quad (9)$$

with $f(k, t) = \int_{-\infty}^{\infty} dx f(x, t) e^{-ikx}$.

In this scenario we modify Eq. (5) by introducing a time-dependent-order fractional derivative according to Eq. (8),

$$\frac{\partial}{\partial t} p(x, t) = \frac{\partial^{\mu(t)}}{\partial |x|^{\mu(t)}} p(x, t) . \quad (10)$$

The initial and boundary conditions are the usual ones,

$$p(x, 0) = \delta(x) ; \quad p(x \rightarrow \pm\infty, t) = 0 , \quad (11)$$

and taking into account the purpose of the present work, i.e., a crossover between two different regimes, we impose the following asymptotic limits for Eq. (10),

$$\frac{\partial}{\partial t} p(x, t) = \frac{\partial^{\mu_1}}{\partial |x|^{\mu_1}} p(x, t) \quad (t \rightarrow 0), \quad (12)$$

$$\frac{\partial}{\partial t} p(x, t) = \frac{\partial^{\mu_2}}{\partial |x|^{\mu_2}} p(x, t) \quad (t \rightarrow \infty). \quad (13)$$

Now, using Eq. (9), we may perform the Fourier transform of Eq. (10) to obtain

$$\frac{\partial}{\partial t} p(k, t) = -|k|^{\mu(t)} p(k, t), \quad (14)$$

implying on

$$p(x, t) = \frac{1}{2\pi} \int_{-\infty}^{+\infty} dk \exp \left[- \int_0^t |k|^{\mu(t')} dt' \right] e^{ikx}, \quad (15)$$

which recovers the Lévy-distribution solution for μ constant.

Given a form for $\mu(t)$, the integral above may be computed for the time interval $[0, t]$ by employing standard numerical tools. Herein, we followed the time evolution of the distribution in Eq. (15) by making use of the pack *NIntegration* from a symbolic computational software, which plots the numerical solution $p(x, t)$ for chosen times.

As can be noticed, there are multiple forms for $\mu(t)$ that interpolate between the limits given by Eqs. (12) and (13). Herein, we have taken into account two ingredients, common in natural systems, for defining these forms: (i) They should present a time-scale parameter (to be defined below as τ), so that the different regimes may be identified by $t \ll \tau$ and $t \gg \tau$; (ii) They should contemplate some typical situations for the crossover to occur, namely, abruptly and smoothly. Hence, to illustrate crossovers between different regimes, we propose below two distinct recipes for $\mu(t)$, interpolating between the Gaussian ($\mu = 2$) and Lévy ($1 \leq \mu < 2$) regimes. The first one is given by

$$\mu(t) = 2\theta \left(1 - \frac{t}{\tau} \right) + \frac{\Gamma + 1}{2} \left(1 + e^{-\frac{t}{\tau}} \right) \theta \left(\frac{t}{\tau} - 1 \right), \quad (16)$$

where Γ is a real parameter in the range from unit to $(3 - e^{-1})/(1 + e^{-1}) \approx 1.924$ (i.e., $\Gamma \in [1, 1.924]$). Due to the Heaviside function $\theta(y)$, this proposal is expected to cover abrupt changes between the two regimes; the second one (which should cover smooth changes) is defined by

$$\mu(t) = 2 - \gamma e^{-\frac{t}{\tau}}, \quad (17)$$

where γ is a real parameter ($\gamma \in (0, 1]$). In both cases τ plays the role of a relaxation time, and herein it will be related, in most cases, to the crossover

time, i.e., $t_{\text{cross}} \propto \tau$. Although these proposals are only illustrative, the changes between the two limiting behaviors, μ_1 ($t \ll \tau$) and μ_2 ($t \gg \tau$), occur more abruptly (smoothly) in Eq. (16) [Eq. (17)], thus covering two distinct physical situations.

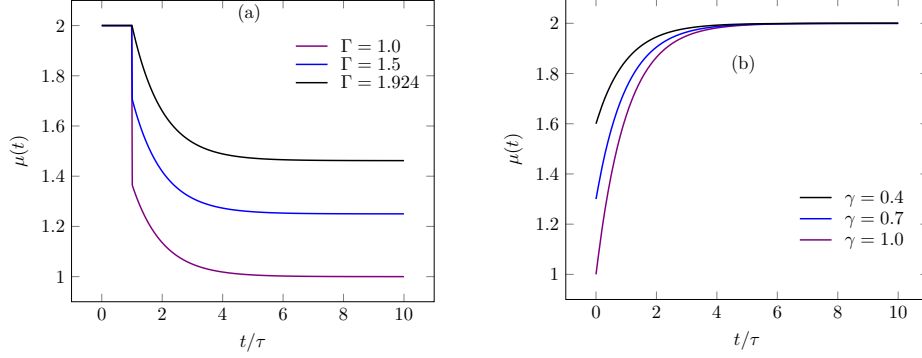


Figure 1: The time-dependent order of the fractional derivative $\mu(t)$ [cf. Eq. (10)] is represented versus time (conveniently rescaled by the crossover time τ): (a) Following Eq. (16) for typical values of the parameter Γ (increasing values of Γ from bottom to top); (b) Following Eq. (17) for typical values of γ (increasing values of γ from top to bottom).

The time evolution of $\mu(t)$ is shown in Fig. 1 for both cases of Eq. (16) [Fig. 1(a)] and Eq. (17) [Fig. 1(b)]. In Fig. 1(a) one finds crossovers between the Gaussian [$\mu(t) = 2$, for $t < \tau$] and typical Lévy [$\mu(t) = (\Gamma + 1)/2$, for $t \gg \tau$] regimes. On the other hand, in Fig. 1(b) crossovers between distinct Lévy regimes [$\mu(t) = 2 - \gamma$, for $t < \tau$] to the Gaussian [$\mu(t) = 2$, for $t \gg \tau$] are exhibited. Although in both cases the crossovers in $\mu(t)$ take place typically in the time interval $\tau < t < 5\tau$, so that for $t > 5\tau$ the final regime has been fully attained, the changes in Fig. 1(a) are more abrupt than those found in Fig. 1(b), as expected. However, as will be shown next, crossovers in the corresponding distributions require much larger times to occur.

Analyzing Eq. (2) one figures out a convenient way for plotting a Gaussian distribution, i.e., through a representation in the rescaled variables, $t^{1/2}p(x, t)$ versus $xt^{-1/2}$, which takes into account the following aspects: (i) Its norm is preserved; (ii) It becomes width-independent, so that Gaussian distributions characterized by different widths all collapse into a single curve. Based on this, we use this representation in Fig. 2, where a Gaussian distribution appears either as the initial [Fig. 2(a)], or long-time distribution [Fig. 2(b)].

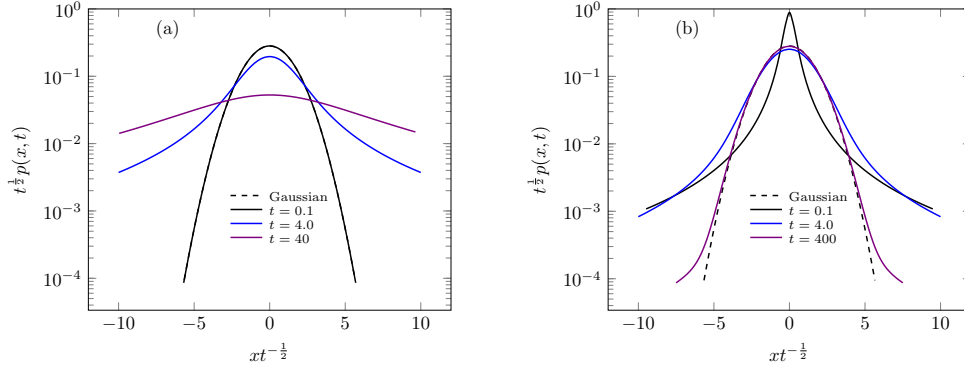


Figure 2: The probability distributions $p(x, t)$ are exhibited (using conveniently rescaled variables) in log-linear representations, for typical times. (a) $\mu(t)$ following Eq. (16) for $\Gamma = 1$ and $\tau = 10$, showing longer tails for increasing times; the case $t = 0.1$ appears superposed with the Gaussian. (b) $\mu(t)$ following Eq. (17) for $\gamma = 1$ and $\tau = 10$, exhibiting shorter tails for increasing times; the case $t = 0.1$ is typically a Cauchy distribution.

In these figures, curves for typical times are shown, where each curve is represented by considering its own time variable t . Therefore, in Fig. 2 we show $p(x, t)$ for increasing times, with the time-dependent order of the fractional derivative following Eq. (16) with $\Gamma = 1$ [panel (a)], and Eq. (17) with $\gamma = 1$ [panel (b)], considering $\tau = 10$ in both cases. In Fig. 2(a) one expects a crossover between the Gaussian ($t \ll \tau$) and Cauchy ($t \gg \tau$) distributions; although the times considered ($0 \leq t \leq 4\tau$) show clearly the crossover region (still far from the long-time regime), one notices the spreading of the distribution towards the expected long-tailed Cauchy distribution. On the other hand, in Fig. 2(b) we present the crossover between the Cauchy ($t \ll \tau$) and Gaussian ($t \gg \tau$) distributions; one notices that the approach to the Gaussian distribution (represented by the dashed curve) appears first around the central region of the distribution. Although the convergence to this limit distribution is expected, the disappearance of the long tails requires larger computational times, in such a way that the probability distribution at $t = 40\tau$ is still different from a Gaussian.

The probability at the origin $p(0, t)$ (also known as return probability) has shown to provide important information about Lévy processes. In fact, according to Eq. (6) one has that

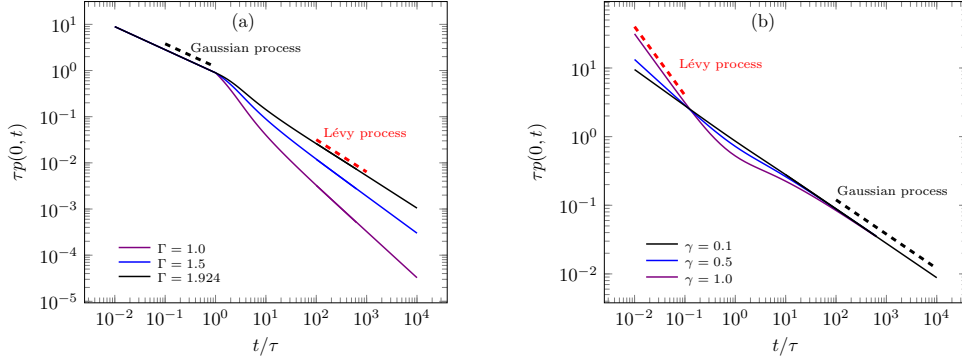


Figure 3: The return probabilities $p(0, t)$ are plotted versus time (using conveniently rescaled variables) in log-log representations, considering $\tau = 10$. (a) $\mu(t)$ following Eq. (16) for typical values of the parameter Γ (in the Lévy regime, increasing values of Γ from bottom to top). (b) $\mu(t)$ following Eq. (17) for typical values of the parameter γ (in the Lévy regime, increasing values of γ from bottom to top). Away from the crossover region, the scaling of Eq. (18) is fulfilled, so that crossovers between the Gaussian ($\mu(t) = 2$) to different Lévy processes with $\mu(t) = (\Gamma + 1)/2$ are verified in (a), whereas crossovers between Lévy processes with $\mu(t) = 2 - \gamma$ to $\mu(t) = 2$ occur in (b).

$$p(0, t) \sim t^{-1/\mu}, \quad (18)$$

in such a way that crossovers between distinct Lévy regimes have been studied in the literature by making use of the above scaling for the return probability [52, 71, 72, 73].

Following this procedure, in Fig. 3 we exhibit the return probability $p(0, t)$ versus time in log-log representations, using conveniently rescaled variables, and setting $\tau = 10$. In Fig. 3(a) we considered $\mu(t)$ following Eq. (16), for typical values of Γ , whereas in Fig. 3(b) we used $\mu(t)$ according to Eq. (17) with different values of γ . These figures suggest that τ is related to a typical time required for a crossover to occur; moreover, away from the crossover region, the scaling of Eq. (18) is fulfilled. One finds changes between the Gaussian ($\mu(t) = 2$) to different Lévy processes with $\mu(t) = (\Gamma + 1)/2$ in Fig. 3(a), as well as between Lévy processes with $\mu(t) = 2 - \gamma$ to $\mu(t) = 2$ in Fig. 3(b). In a similar way, in Fig. 4 we present $p(0, t)$ for several values of τ , fixing $\Gamma = 1$ [Fig. 4(a)] and $\gamma = 1$ [Fig. 4(b)]; these results reinforce

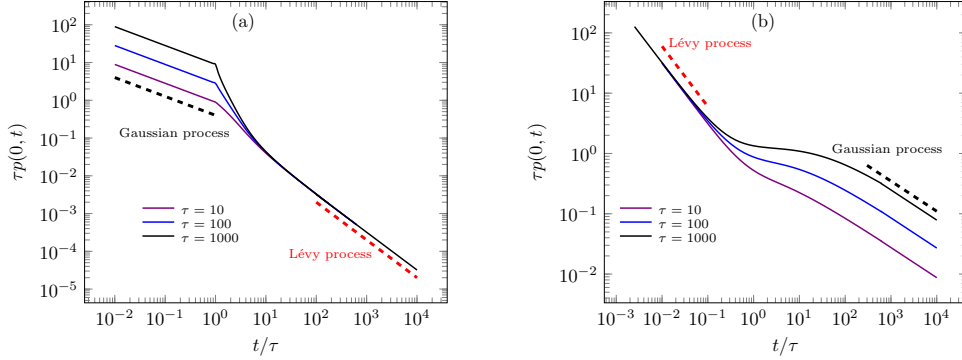


Figure 4: The return probabilities $p(0, t)$ are plotted versus time (using conveniently rescaled variables) in log-log representations for typical values of τ . (a) $\mu(t)$ following Eq. (16) for $\Gamma = 1$ (in the Gaussian regime, increasing values of τ from bottom to top). (b) $\mu(t)$ following Eq. (17) for $\gamma = 1$ (in the Gaussian regime, increasing values of τ from bottom to top). Away from the crossover region, the scaling of Eq. (18) is fulfilled, so that crossovers between Gaussian ($\mu(t) = 2$) to Lévy ($\mu(t) = 1$) processes are verified in (a), whereas crossovers between Lévy ($\mu(t) = 1$) to Gaussian ($\mu(t) = 2$) processes with occur in (b).

the proposal that τ should be related to the crossover time, i.e., $t_{\text{cross}} \propto \tau$. One observes crossovers between the Gaussian ($\mu = 2$) to a Cauchy distribution ($\mu = 1$) in Fig. 4(a), whereas those between the Cauchy and Gaussian distributions are found in Fig. 4(b). As expected, in both Figs. 3 and 4 one notices that the crossovers occur more abruptly in cases following Eq. (16) [typically in the time intervals $1 < (t/\tau) < 10$ in Figs. 3(a) and 4(a)], than those of Eq. (17) [typically in the time intervals $10^{-1} < (t/\tau) < 10^2$ in Figs. 3(b) and 4(b)], thus covering two possible distinct real situations.

As will be discussed later, the model defined above should be applicable to processes presenting slow variations on its relevant environmental parameters, leading to smooth variations on the exponent $\mu(t)$. In such cases, intermediate Lévy processes should appear, characterized by $\mu_1 \leq \mu(t) \leq \mu_2$. As candidates, one mentions a new optical material constructed from glass microspheres, so-called Lévy glass [38], light scattering in atomic vapours [74], and cold atoms in optical lattices [75].

2.2. Model 2: Time-Dependent Diffusion Coefficients

The second model that we investigate consists in modifying Eq. (5) by introducing two competing diffusive contributions, characterized by different time-dependent diffusion coefficients, as follows

$$\frac{\partial}{\partial t}p(x, t) = \mathcal{K}_1(t) \frac{\partial^{\mu_1}}{\partial |x|^{\mu_1}} p(x, t) + \mathcal{K}_2(t) \frac{\partial^{\mu_2}}{\partial |x|^{\mu_2}} p(x, t) . \quad (19)$$

To obtain crossovers between two Lévy processes one may consider the above time-dependent diffusion coefficients leading to a prevalence of one of the fractional Laplacian terms at different time regimes, e.g., $\lim_{t \rightarrow 0} \mathcal{K}_1(t) = 1$ and $\lim_{t \rightarrow 0} [\mathcal{K}_2(t)/\mathcal{K}_1(t)] = 0$, together with $\lim_{t \rightarrow \infty} [\mathcal{K}_1(t)/\mathcal{K}_2(t)] = 0$ and $\lim_{t \rightarrow \infty} \mathcal{K}_2(t) = 1$. These choices lead to the same limits specified in Eqs. (12) and (13), so that $p(x, t) \propto L_{\mu_1}(x, t)$ ($t \rightarrow 0$), whereas $p(x, t) \propto L_{\mu_2}(x, t)$ ($t \rightarrow \infty$).

Following the usual procedure, Eq. (19) may be handled by performing a Fourier transform, leading to

$$\frac{\partial}{\partial t}p(k, t) = -[\mathcal{K}_1(t)|k|^{\mu_1} + \mathcal{K}_2(t)|k|^{\mu_2}]p(k, t) , \quad (20)$$

which admits the solution,

$$p(k, t) = A(k)\varphi(k, t), \quad (21)$$

where

$$\varphi(k, t) = \exp \left[-|k|^{\mu_1} \int_0^t dt' \mathcal{K}_1(t') - |k|^{\mu_2} \int_0^t dt' \mathcal{K}_2(t') \right] , \quad (22)$$

and $A(k)$ is an arbitrary function in Fourier space. Using the conditions of Eq. (11) one obtains

$$p(x, t) = \frac{1}{2\pi} \int_{-\infty}^{+\infty} dk \varphi(k, t) e^{-ikx} . \quad (23)$$

In this way, the solution becomes a convolution of Lévy distributions,

$$p(x, t) = \frac{1}{\mathcal{P}_{\mu_1, \mu_2}(t)} \int_{-\infty}^{\infty} dx' L_{\mu_1} \left[\frac{|x - x'|}{\left(\int_0^t dt' \mathcal{K}_1(t') \right)^{\frac{1}{\mu_1}}} \right] L_{\mu_2} \left[\frac{|x'|}{\left(\int_0^t dt' \mathcal{K}_2(t') \right)^{\frac{1}{\mu_2}}} \right], \quad (24)$$

where

$$\mathcal{P}_{\mu_1, \mu_2}(t) = \left(\int_0^t dt' \mathcal{K}_1(t') \right)^{\frac{1}{\mu_1}} \left(\int_0^t dt' \mathcal{K}_2(t') \right)^{\frac{1}{\mu_2}}. \quad (25)$$

As done previously in the solution of Eq. (15), we used the pack *NIntegration* to follow the time evolution of the distribution in Eq. (24), for given $\mathcal{K}_1(t)$ and $\mathcal{K}_2(t)$. In this way, we illustrate below the crossovers exhibited by the present model through the numerical integration of the probability distribution in Eq. (24), by defining the time-dependent diffusion coefficients of Eq. (19) as

$$\mathcal{K}_1(t) = e^{-\frac{t}{\tau}} \quad \text{and} \quad \mathcal{K}_2(t) = 1 - e^{-\frac{t}{\tau}}, \quad (26)$$

which satisfy the limits established in Eqs. (12) and (13).

For the same reasons mentioned before in Fig. 2, we consider the rescaled variables $t^{1/2}p(x, t)$ versus $xt^{-1/2}$ in Fig. 5, which turn out to be convenient in the two Gaussian limits, namely, the initial [Fig. 5(a)], and long-time distributions [Fig. 5(b)]. Hence, in Fig. 5 we represent $p(x, t)$ (using these conveniently rescaled variables) for increasing times, by considering the proposal of Eq. (19), with the time-dependent diffusion coefficients defined according to Eq. (26). These plots were obtained through a numerical integration of Eq. (24) for $\tau = 10$ and typical values of t . Two situations are exhibited, namely, crossovers between the Gaussian and Cauchy distributions [panel (a)], as well as between the Cauchy and Gaussian [panel (b)]. In Fig. 5(a) one notices that deviations from the Gaussian behavior start in the tails, whereas the central part persists longer, as shown in the curve for $t = 0.4\tau$; on the hand, the distribution at time $t = 2\tau$ is essentially inside the crossover interval between the two regimes. In a similar manner, in Fig. 5(b) one sees that $p(x, t)$ for $t = \tau$ is typically inside the crossover time interval, whereas for a much larger time ($t = 4 \times 10^3 \tau$), the central part of the distribution has essentially converged to the Gaussian, although significant discrepancies

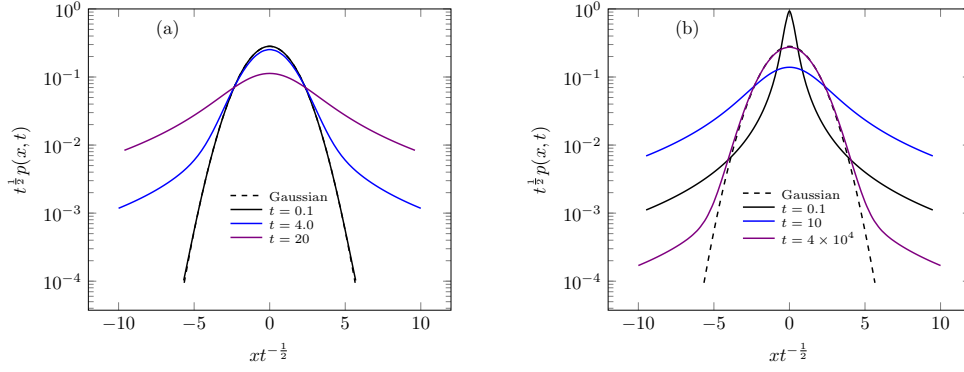


Figure 5: The probability distributions $p(x, t)$ are exhibited (using conveniently rescaled variables) in log-linear representations, for typical times. These distributions change in time following the model characterized by two different time-dependent diffusion coefficients [cf. Eq. (19)], defined according to Eq. (26), with $\tau = 10$. (a) Time evolution between the Gaussian (represented by a dashed line, superposed with curve for $t = 0.1$) and Cauchy distributions, i.e., $\mu_1 = 2$ ($t = 0$) to $\mu_2 = 1$ ($t \rightarrow \infty$), showing longer tails for increasing times; (b) Time evolution between the Cauchy and Gaussian (represented by the dashed line) distributions, i.e., $\mu_1 = 1$ ($t = 0$) to $\mu_2 = 2$ ($t \rightarrow \infty$), exhibiting shorter tails for increasing times.

persist in the tails, requiring even longer times for disappearing. This later behavior has already been observed in the previous model, characterized by a time-dependent order of the fractional derivative, in which the convergence to the final distribution requires longer times for accommodating its long tails. Since both models satisfy the limits established in Eqs. (12) and (13), the final distribution should be attained after sufficiently long times; however, by comparing Figs. 2(b) and 5(b) one concludes that the disappearance of the tails requires larger times in model 2.

In Fig. 6 we present the return probability $p(0, t)$ versus time in log-log representations, considering the model defined in Eq. (19), with the time-dependent diffusion coefficients following Eq. (26), for typical values of τ ; these plots were obtained by a numerical integration of Eq. (24) for $x = 0$. The crossover regions occur typically in the time intervals $10^{-1} < (t/\tau) < 10$ [Fig. 6(a)] and $10^{-1} < (t/\tau) < 10^2$ [Fig. 6(b)], showing that the approach to the Gaussian limit requires larger times, in agreement with Fig. 5(b). One notices that away from the crossover region, the scaling of Eq. (18) is fulfilled, with Fig. 6(a) showing a Gaussian regime ($\mu = 2$) for $t \ll \tau$,

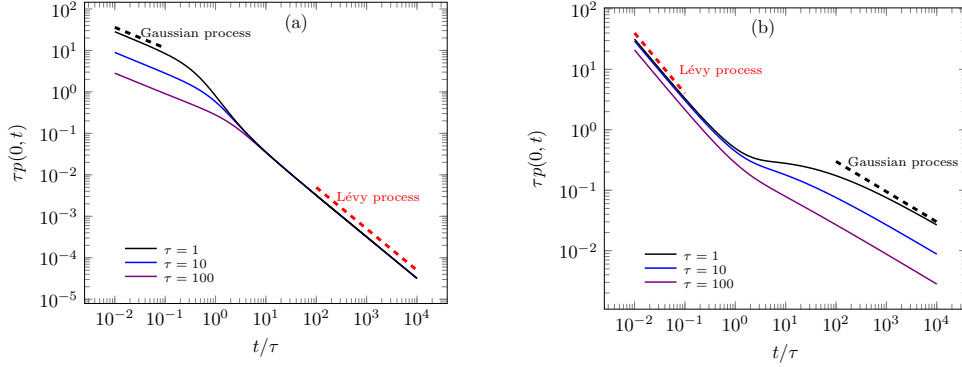


Figure 6: The return probabilities $p(0, t)$ are plotted versus time (using conveniently rescaled variables) in log-log representations, for typical values of τ , following the model characterized by two different time-dependent diffusion coefficients [cf. Eq. (19)], defined according to Eq. (26). Away from the crossover region, the scaling of Eq. (18) is fulfilled, so that a crossover between the Gaussian ($\mu = 2$) to a Cauchy distribution ($\mu = 1$) is verified in (a), and between a Cauchy and the Gaussian occurs in (b). In the Gaussian regime, increasing values of τ apply to curves from top to bottom.

whereas a Cauchy behavior occurs for $t \gg \tau$; an inverse crossover is observed in Fig. 6(b). By comparing Figs. 4(b) and 6(b) one sees that the present model yields results qualitatively similar to those of model 1, i.e., a smooth change between the two regimes, when considering the former model with $\mu(t)$ following Eq. (17).

One important comment concerns the changes associated with the distribution tails, like shown in Fig. 5(b), where the central part of the distribution has converged to the Gaussian, although significant discrepancies persist in the tails up to a time $t = 4 \times 10^3 \tau$. One should mention that such a behavior, where the central part converges faster than the tails, is very common in long-tailed-distribution studies (see, e.g., Ref [17]). By comparing the largest-time distribution in Fig. 5(b) with the corresponding curve in Fig. 6(b) (cf. case $\tau = 10$), one sees that the convergence to the Gaussian limit provided by the analysis of the return probability $p(0, t)$ [which occurs for $t \simeq 10^2 \tau$ in Fig. 6(b)] is incomplete, since this approach focuses only in the time evolution of the central part of the distribution. In such cases, appropriate numerical procedures, taking into account the time evolution of the whole distribution should be carried; as an example where this type of approach

has been developed, we mention the investigation of the time evolution of q -Gaussian distributions, as solutions of the porous-medium equation, carried in Ref [17]. However, this type of procedure falls out of the scope of the present study.

The model defined in Eq. (19), which consists essentially in a superposition of two distributions at each time t (except for the limits $t \rightarrow 0$ and $t \rightarrow \infty$), is expected to be useful for describing real systems, like the diffusion of particles in *cytoskeleton* of a cell [77]. Moreover, a superposition of Gaussian and Lévy distributions was investigated in the competition problem of two species [78].

3. Conclusions

To sum up, we have proposed two models capable of producing crossovers among Lévy flights, characterized by distinct diffusion exponents. The first one (called model 1) considers a time-dependent-order Riesz fractional derivative in the Laplacian term of the diffusion equation, whereas the second one (named model 2) is defined by two fractional-derivative diffusive terms, each of them multiplied by different time-dependent diffusion coefficients. We have investigated these models by analytical calculations, followed by numerical integrations, for obtaining the corresponding distributions $p(x, t)$. Although both yield the desired crossovers, attaining the expected limits for sufficiently long times, the crossovers may occur in qualitatively different ways, due to the fact that model 1 is characterized by a single Lévy process at each time t , with a time-varying exponent $\mu(t)$, whereas in model 2 the distribution at time t is expressed in terms of a convolution of two Lévy processes, each with its own exponent. Typical crossovers among distinct Lévy processes are illustrated for both cases, by following numerically the time evolution of the resulting distribution $p(x, t)$, as well as by monitoring the scaling on time of the return probability, $p(0, t) \sim t^{-1/\mu}$.

One should mention that crossovers among distinct types of anomalous diffusion, characterized by different diffusion exponents, have been observed often in nature, although proposals of theoretical models for describing such effects are very rare in the literature. As an example, one has the model introduced recently in Ref. [79], based on the theory of continuous-time random walks; this model differs from the present ones, in the sense that it leads to a diffusion equation characterized by a time-fractional derivative, whereas in the present case (model 1) one has a time-dependent-order fractional deriva-

tive in the Laplacian term of the diffusion equation. Moreover, a convolution of two Lévy distributions at a given time t , as introduced herein in model 2, is significantly different from the proposal of Ref. [79].

The crossovers described in the previous section, particularly those between Lévy and Gaussian distributions, have been observed in a class of stochastic processes, the so-called truncated Lévy flights [52], in econophysical applications, like in the behavior of commodity-price distributions [72], as well as in the analysis of experimental data in tokamak edge turbulence of plasmas [76], among many other systems.

A major question concerns which kind of theoretical model should be more appropriate for describing a specific crossover observed. As expected, both models presented are able to drive systems from the initial Lévy process, characterized by an exponent μ_1 , to the final one, described by an exponent μ_2 . The essential differences between these models appear in their crossover mechanisms. In model 1 the crossover occurs through a gradual change in the exponent $\mu(t)$, so that in the crossover region the system is expected to approach different Lévy regimes, for given time intervals, with $\mu_1 \leq \mu(t) \leq \mu_2$. In this crossover regime, slow changes in relevant quantities of the environment, like temperature, diffusivity, and viscosity, should lead to slightly different Lévy flights; therefore, model 1 would be useful to investigate experimental systems in which different Lévy processes may occur due to gradual changes on environmental properties. On the other hand, a superposition of two Riesz operators, considered in model 2, also yields a crossover between two distinct Lévy processes, characterized by exponents μ_1 and μ_2 . However, in this case, typical ingredients and properties of both processes are present during the whole crossover interval, so that in different time regimes, one Lévy process becomes more relevant than the other one. Differently from the first case, model 2 is expected to present a crossover without exploring intermediate Lévy flights (which may occur between the initial and final distributions), but should rather present combinations of the two processes.

Hence, considering the reasons explained above, one should mention that systems characterized by slowly varying properties, like light scattering in a new optical material constructed from glass microspheres, so-called Lévy glass [38], light scattering in atomic vapours [74], and cold atoms in optical lattices [75] are good candidates for model 1. On the other hand, model 2, which consists essentially in a superposition of two distributions at each time t , is expected to be useful for describing the diffusion of particles in

cytoskeleton of a cell [77], as well as for a two-species competition problem, where a superposition of Gaussian and Lévy distributions has been considered [78]. Additionally, model 2 should also be relevant in the context of foraging process, to investigate random search models that consider a combination of two Lévy processes to study search strategies [80]. In general, situations where two species of living beings compete with each other, leading to some time of crossover, like in food searching, physical-space disputes, among other situations, become appropriate candidates for model 2.

In some cases, it may not be obvious to point out a priori which model would be more appropriate for describing specific applications, and there may be situations where both (or neither) of them become suitable. For these, as often occurs with theoretical proposals, only through comparison with experimental data, one should be able to choose from one of these models. However, due to their general characteristics and potential of applicability in different contexts, the present proposals should cover many classes of real phenomena involving crossovers among distinct Lévy processes.

Acknowledgements

The authors thank C. Tsallis for fruitful conversations. M.A.F. dos Santos acknowledges support from the Brazilian agency CAPES (INCT-SC). F.D. Nobre and E.M.F. Curado acknowledge partial financial support from CNPq, CAPES, and FAPERJ (Brazilian funding agencies).

References

- [1] Reichl L. *A Modern Course in Statistical Physics*, Second edition. John Wiley and Sons New York, 1998.
- [2] Krapivsky PL, Redner S, Ben-Naim E. *A Kinetic View of Statistical Physics*, Second edition. Cambridge University Press Cambridge, 2010.
- [3] Tsallis C. Lévy distributions. *Physics World*, 10(7):42, 1997.
- [4] Tsallis C. *Introduction to Nonextensive Statistical Mechanics*, Springer New York, 2009.
- [5] Tsallis C. An introduction to nonadditive entropies and a thermostatical approach to inanimate and living matter. *Contemporary Physics*, 55:179, 2014.

- [6] Sposini V, Chechkin AV, Seno F, Pagnini G, Metzler R. Random diffusivity from stochastic equations: comparison of two models for Brownian yet non-Gaussian diffusion. *New Journal of Physics*, 20(4):043044, 2018.
- [7] Chechkin AV, Seno F, Metzler R, Sokolov I M. Brownian yet non-Gaussian diffusion: from superstatistics to subordination of diffusing diffusivities. *Physical Review X*, 7(2):021002, 2017.
- [8] Slkezak J, Metzler R, Magdziarz M. Superstatistical generalised Langevin equation: non-Gaussian viscoelastic anomalous diffusion. *New J. Phys.*, 20(2):023026, 2018.
- [9] Santos MAF. Non-Gaussian distributions to random walk in the context of memory kernels. *Fractal and Fractional*, 2(3):20, 2018.
- [10] Santos MAF. Fractional Prabhakar derivative in diffusion equation with non-static stochastic resetting. *Physics*, 1(1):40–58, 2019.
- [11] Hristov J. Response functions in linear viscoelastic constitutive equations and related fractional operators. *Math. Model. Nat. Phenom.*, 14(3):305, 2019.
- [12] Santos MAF. From continuous-time random walks to controlled-diffusion reaction. *Journal of Statistical Mechanics: Theory and Experiment*, 2019(3):033214, 2019.
- [13] Reid BA, Täuber UC, Brunson JC. Reaction-controlled diffusion: Monte Carlo simulations. *Phys. Rev. E*, 68:046121, Oct 2003.
- [14] Santos MAF. A fractional diffusion equation with sink term. *Indian Journal of Physics*, 2019.
- [15] Rebenshtok A, Denisov S, Hänggi P, Barkai E. Complementary densities of Lévy walks: typical and rare fluctuations. *Math. Model. Nat. Phenom.*, 11(3):76–106, 2016.
- [16] Wang W, Schulz JHP, Deng W, Barkai E. Renewal theory with fat-tailed distributed sojourn times: Typical versus rare. *Physical Review E*, 98(4):042139, 2018.

- [17] Schwämmle V, Nobre FD, Tsallis C. q-Gaussians in the porous-medium equation: stability and time evolution. *Eur. Phys. J. B*, 66(4):537–546, 2008.
- [18] Plastino AR, Plastino A. Non-extensive statistical mechanics and generalized Fokker-Planck equation. *Physica A* 222:347, 1995.
- [19] Tsallis C, Bukman DJ. Anomalous diffusion in the presence of external forces: Exact time-dependent solutions and their thermostistical basis. *Phys. Rev. E* 54:R2197, 1996.
- [20] Schwämmle V, Curado EMF, Nobre FD. Dynamics of normal and anomalous diffusion in nonlinear Fokker-Planck equations. *Eur. Phys. J. B*, 70(1):107–116, 2009.
- [21] Curado EMF, Nobre FD. Equilibrium states in two-temperature systems. *Entropy*, 20(3):183, 2018.
- [22] Casas GA, Nobre FD. Nonlinear Fokker-Planck equations in super-diffusive and sub-diffusive regimes. *J. Math. Phys.*, 60(5):053301, 2019.
- [23] Troncoso P, Fierro O, Curilef S, Plastino AR. A family of evolution equations with nonlinear diffusion, Verhulst growth, and global regulation: Exact time-dependent solutions. *Physica A* 375:457–466. 2007.
- [24] Metzler R, Klafter J. The random walk’s guide to anomalous diffusion: a fractional dynamics approach. *Phys. Rep.*, 339(1):1–77, 2000.
- [25] Metzler R, Jeon JH, Cherstvy A, Barkai E. Anomalous diffusion models and their properties: non-stationarity, non-ergodicity, and ageing at the centenary of single particle tracking. *Phys. Chem. Chem. Phys.*, 16(44):24128–24164, 2014.
- [26] Santos MAF. Analytic approaches of the anomalous diffusion: A review. *Chaos, Solitons & Fractals*, 124:86–96, 2019.
- [27] Lévy P, Borel M. *Théorie de l’addition des variables aléatoires*, volume 1. Gauthier-Villars Paris, 1954.
- [28] Zaburdaev V, Denisov S, Klafter J. Lévy walks. *Rev. Mod. Phys.*, 87(2):483, 2015.

- [29] Bertoin J. *Lévy processes*, volume 121. Cambridge University Press Cambridge, 1996.
- [30] Nolan J. *Stable distributions: models for heavy-tailed data*. Birkhauser New York, 2003.
- [31] Gnedenko BV, Kolmogorov A. *Limit distributions for sums of independent random variables*. *Am. J. Math.*, 105, 1954.
- [32] Tsallis C, Levy SVF, Souza AMC, Maynard R. Statistical-Mechanical Foundation of the Ubiquity of Lévy Distributions in Nature. *Phys. Rev. Lett.*, 75:3589, 1995.
- [33] Montroll EW, Weiss GH. Random walks on lattices. ii. *J. Math. Phys.*, 6(2):167–181, 1965.
- [34] Scher H, Montroll EW. Anomalous transit-time dispersion in amorphous solids. *Phys. Rev. B*, 12(6):2455, 1975.
- [35] Scher H, Montroll EW. Random walks on lattices. iv. continuous-time walks and influence of absorbing boundaries. *J. Stat. Phys.*, 9(2):101–135, 1973.
- [36] Laskin N. Fractional Schrödinger equation. *Phys. Rev. E*, 66(5):056108, 2002.
- [37] Stefano Longhi. Fractional Schrödinger equation in optics. *Opt. Lett.*, 40(6):1117–1120, 2015.
- [38] Barthélemy P, Bertolotti J, Wiersma DS. A Lévy flight for light. *Nature*, 453(7194):495, 2008.
- [39] Barkai E. Stable equilibrium based on Lévy statistics: Stochastic collision models approach. *Phys. Rev. E*, 68:055104, 2003.
- [40] Barkai E. Stable equilibrium based on Lévy statistics: a linear Boltzmann equation approach. *J. Stat. Phys.*, 115(5-6):1537–1565, 2004.
- [41] Vezzani A, Barkai E, Burioni R. Single-big-jump principle in physical modeling. *Phys. Rev. E*, 100:012108, 2019.

- [42] Aghion E, Kessler DA, Barkai E. Large fluctuations for spatial diffusion of cold atoms. *Phys. Rev. Lett.*, 118(26):260601, 2017.
- [43] Kumierz L, Gudowska-Nowak E. Optimal first-arrival times in Lévy flights with resetting. *Phys. Rev. E*, 92:052127, 2015.
- [44] Lomholt MA, Ambjörnsson T, Metzler R. Optimal target search on a fast-folding polymer chain with volume exchange. *Phys. Rev. Lett.*, 95(26):260603, 2005.
- [45] Blainey PC, Oijen AMV, Banerjee A, Verdine GL, Xie XS. A base-excision DNA-repair protein finds intrahelical lesion bases by fast sliding in contact with DNA. *Proc. Nat. Acad. Sci.*, 103(15):5752–5757, 2006.
- [46] Bronstein I, Israel Y, Kepten, Mai ES, Tal YS, Barkai E, Garini Y. Transient anomalous diffusion of telomeres in the nucleus of mammalian cells. *Phys. Rev. Lett.*, 103:018102, 2009.
- [47] Höfling F, Franosch T. Anomalous transport in the crowded world of biological cells. *Rep. Prog. Phys.*, 76(4):046602, 2013.
- [48] Garcia DM, Sandev T, Hadiseh Safdari, Pagnini G, Chechkin A, Metzler R. Crossover from anomalous to normal diffusion: truncated power-law noise correlations and applications to dynamics in lipid bilayers. *New J. Phys.*, 20(10):103027, 2018.
- [49] Stanislavsky A, Weron A. Control of the transient subdiffusion exponent at short and long times. *Phys. Rev. Research*, 1:023006, 2019.
- [50] Inoue J, Sazuka N. Crossover between Lévy and Gaussian regimes in first-passage processes. *Phys. Rev. E*, 76:021111, 2007.
- [51] Spagnolo B, Valenti D. Volatility effects on the escape time in financial market models. *International Journal of Bifurcation and Chaos*, 18(09):2775–2786, 2008.
- [52] Mantegna RN, Stanley HE. Stochastic process with ultraslow convergence to a Gaussian: the truncated Lévy flight. *Phys. Rev. Lett.*, 73(22):2946, 1994.
- [53] Santos MAF. Mittag-Leffler memory kernel in Lévy flights. *Mathematics*, 7(9):766, 2019.

- [54] Lorenzo CF, Hartley TT. Variable order and distributed order fractional operators. *Nonlinear dynamics*, 29(1-4):57–98, 2002.
- [55] Lorenzo CF, Hartley TT. Initialization, conceptualization, and application in the generalized (fractional) calculus. *Critical Reviews in Biomedical Engineering*, 35(6), 2007.
- [56] Sun HG, Chen W, Chen Y. Variable-order fractional differential operators in anomalous diffusion modelling. *Physica A*, 388(21):4586–4592, 2009.
- [57] Yang XJ, Machado JAT. A new fractional operator of variable order: application in the description of anomalous diffusion. *Physica A*, 481:276–283, 2017.
- [58] Sun HG, Chen W, Wei H, Chen YQ. newblock A comparative study of constant-order and variable-order fractional models in characterizing memory property of systems. *Eur. Phys. J. Spec. Top.*, 193(1):185, 2011.
- [59] Hajipour M, Jajarmi A, Baleanu D, Sun H. On an accurate discretization of a variable-order fractional reaction-diffusion equation. *Commun. Nonlinear Sci. Numer. Simul.* 69:119–133, 2019.
- [60] Heydari MH, Avazzadeh Z, Yang Y. A computational method for solving variable-order fractional nonlinear diffusion-wave equation. *Appl. Math. Comput.*, 352:235–248, 2019.
- [61] Aguilar JFG, Atangana A. Time-fractional variable-order telegraph equation involving operators with Mittag-Leffler kernel. *J. Electromagn. Waves Appl.*, 33(2):165–177, 2019.
- [62] Hosseininia M, Heydari MH. Meshfree moving least squares method for nonlinear variable-order time fractional 2d telegraph equation involving Mittag-Leffler non-singular kernel. *Chaos, Solitons & Fractals*, 127:389–399, 2019.
- [63] Almeida R, Tavares D, Torres DFM, *The variable-order fractional calculus of variations*. Springer, 2019.
- [64] Ortigueira MD, Valério D, Machado JT. Variable order fractional systems. *Comm. Nonlinear Sci. Numer. Simulat.*, 71:231–243, 2019.

- [65] Dabiri A, Moghaddam BP, Machado JAT. Optimal variable-order fractional pid controllers for dynamical systems. *J. Comput. Appl. Math.*, 339:40 – 48, 2018.
- [66] Fu ZJ, Chen W, Ling L. Method of approximate particular solutions for constant- and variable-order fractional diffusion models. *Eng. Anal. Bound. Elem.*, 57:37 – 46, 2015.
- [67] Sun HG, Chang C A, Zhang Y, Chen W. A review on variable-order fractional differential equations: mathematical foundations, physical models, numerical methods and applications. *Fract. Calc. Appl. Anal.*, 22(1):27–59, 2019.
- [68] Chechkin AV, Gorenflo R, Sokolov IM. Fractional diffusion in inhomogeneous media. *J. Phys. A*, 38(42), L679, 2005.
- [69] Zhuang P, Liu F, Anh V, Turner I. Numerical methods for the variable-order fractional advection-diffusion equation with a nonlinear source term. *SIAM J. Numer. Anal.*, 47(3):1760–1781, 2009.
- [70] Lin R, Liu F, Anh V, Turner I. Stability and convergence of a new explicit finite-difference approximation for the variable-order nonlinear fractional diffusion equation. *Appl. Math. Comput.*, 212(2):435–445, 2009.
- [71] Koponen I. Analytic approach to the problem of convergence of truncated Lévy flights towards the Gaussian stochastic process. *Phys. Rev. E*, 52:1197–1199, 1995.
- [72] Sokolov IM, Chechkin AV, Klafter J. Fractional diffusion equation for a power-law-truncated Lévy process. *Physica A*, 336(3-4):245–251, 2004.
- [73] Chechkin AV, Metzler R, Klafter J, Gonchar VY. Introduction to the theory of Lévy flights. *Anomalous transport: Foundations and applications*, 49(2):431–451, 2008.
- [74] Mercadier N, Chevroliier M, Guerin W, Kaiser R. Microscopic characterization of Lévy flights of light in atomic vapours. *Physical Review A*, 87(6), 063837, 2013.

- [75] Kessler DA, Barkai E. Theory of fractional Lévy kinetics for cold atoms diffusing in optical lattices. *Physical Review Letters*, 108(23), 230602, 2012.
- [76] Jha R, Kaw PK, Kulkarni DR, Parikh JC, Aditya Team. Evidence of Lévy stable process in tokamak edge turbulence, *Phys. Plasmas*, 10(3), 699-704, 2003.
- [77] Alencar AM, Ferraz MSA, Park CY, Millet E, Trepas X, Fredberg JJ, Butler JP. Non-equilibrium cytoquake dynamics in cytoskeletal remodeling and stabilization. *Soft Matter*, 12(41):8506–8511, 2016.
- [78] Heinsalu E, García EH, López C. Spatial clustering of interacting bugs: Lévy flights versus Gaussian jumps. *Europhys. Lett.*, 92(4):40011, 2010.
- [79] Sandev T, Deng W, Xu P. Models for characterizing the transition among anomalous diffusions with different diffusion exponents. *J. Phys. A*, 51(40):405002, 2018.
- [80] Palyulin VV, Mantsevich VN, Klages R, Metzler R, Chechkin AV. Comparison of pure and combined search strategies for single and multiple targets. *The European Physical Journal B*, 90(9), 170, 2017.